NeuroImage 263 (2022) 119624

Contents lists available at ScienceDirect

NeuroImage

journal homepage: www.elsevier.com/locate/neuroimage

Psychedelics and schizophrenia: Distinct alterations to Bayesian inference

Hardik Rajpal[a,b,f,1,*], Pedro A.M. Mediano[c,d,e,1], Fernando E. Rosas[a,g,h,p], Christopher B. Timmermann[g], Stefan Brugger[k,l], Suresh Muthukumaraswamy[m], Anil K. Seth[n,o], Daniel Bor[d,e], Robin L. Carhart-Harris[g,i], Henrik J. Jensen[a,b,j]

[a] Centre for Complexity Science, Imperial College London, South Kensington, London, United Kingdom
[b] Department of Mathematics, Imperial College London, South Kensington, London, United Kingdom
[c] Department of Computing, Imperial College London, South Kensington, London, United Kingdom
[d] Department of Psychology, University of Cambridge, Cambridge, United Kingdom
[e] Department of Psychology, Queen Mary University of London, London, United Kingdom
[f] Public Policy Program, The Alan Turing Institute, London, United Kingdom
[g] Centre for Psychedelic Research, Department of Brain Sciences, Imperial College London, London, United Kingdom
[h] Data Science Institute, Imperial College London, London, United Kingdom
[i] Psychedelics Division, Neuroscape, Department of Neurology, University of California San Francisco, US
[j] Institute of Innovative Research, Tokyo Institute of Technology, Yokohama, Japan
[k] Cardiff University Brain Research Imaging Centre, School of Psychology, Cardiff University, United Kingdom
[l] Centre for Academic Mental Health, Bristol Medical School, University of Bristol, United Kingdom
[m] School of Pharmacy, The University of Auckland, New Zealand
[n] School of Engineering and Informatics, University of Sussex, United Kingdom
[o] CIFAR Program on Brain, Mind, and Consciousness, Toronto, Canada
[p] Department of Informatics, University of Sussex, Brighton, United Kingdom

ARTICLE INFO

Keywords:
Psychedelics
Schizophrenia
Information theory
Predictive processing

ABSTRACT

Schizophrenia and states induced by certain psychotomimetic drugs may share some physiological and phenomenological properties, but they differ in fundamental ways: one is a crippling chronic mental disease, while the others are temporary, pharmacologically-induced states presently being explored as treatments for mental illnesses. Building towards a deeper understanding of these different alterations of normal consciousness, here we compare the changes in neural dynamics induced by LSD and ketamine (in healthy volunteers) against those associated with schizophrenia, as observed in resting-state M/EEG recordings. While both conditions exhibit increased neural signal diversity, our findings reveal that this is accompanied by an increased transfer entropy from the front to the back of the brain in schizophrenia, versus an overall reduction under the two drugs. Furthermore, we show that these effects can be reproduced via different alterations of standard Bayesian inference applied on a computational model based on the predictive processing framework. In particular, the effects observed under the drugs are modelled as a reduction of the precision of the priors, while the effects of schizophrenia correspond to an increased precision of sensory information. These findings shed new light on the similarities and differences between schizophrenia and two psychotomimetic drug states, and have potential implications for the study of consciousness and future mental health treatments.

1. Introduction

Classic serotonergic psychedelic drugs have seen a blooming resurgence among the public and the scientific community in recent years, largely driven by promising clinical research into their therapeutic potential Carhart-Harris et al. (2021, 2017). At the same time, and somewhat paradoxically, psychedelics are known to elicit effects that mimic some symptoms of psychosis – earning them the label of 'psychotomimetic drugs' Carhart-Harris et al. (2016a). In this context, our aims with this study are twofold: First, to explore the limits of psychotomimetic models of psychosis at a neurophysiological level, thus helping us refine these models. Second, to further our understanding of extended and acute alterations to normal consciousness, which may help the design better mental health therapies.

To contrast these conditions in an empirical manner, we compare neuroimaging data from patients suffering from schizophre-

* Corresponding author.
E-mail addresses: h.rajpal15@imperial.ac.uk (H. Rajpal), pmediano@imperial.ac.uk (P.A.M. Mediano).
[1] H.R. and P.M. contributed equally to this work.

https://doi.org/10.1016/j.neuroimage.2022.119624.
Received 10 May 2022; Received in revised form 11 August 2022; Accepted 10 September 2022
Available online 13 September 2022.

nia and healthy subjects under the effects of two psychoactive substances: the classical psychedelic lysergic acid diethylamide (LSD) Carhart-Harris et al. (2016b) and the dissociative drug ketamine (KET) Frohlich and Van Horn (2014).

Using standardised assessments, it has been claimed that KET reproduces both positive and negative symptoms of schizophrenia in humans Beck et al. (2020), and its mechanism of action – NMDA receptor antagonism – is thought to reproduce a key element of the molecular pathophysiology of schizophrenia Friston et al. (2016); McCutcheon et al. (2020). LSD – in common with all classical psychedelics – is a potent agonist of a number of serotonin receptors, but its characteristic effects depend primarily on 5-HT_{2A} Nichols (2004). These neurotransmitter systems have been linked to symptoms of early acute schizophrenic stages, such as "ego-disorders, affective changes, loosened associations and perceptual alterations" Vollenweider et al. (1998) (see Ref. Carhart-Harris et al. (2013) for a quantitative analysis of these associations).

Both psychotomimetic drug states and schizophrenia are also associated with marked changes in large-scale neural dynamics. For both LSD and KET, previous studies have found increased signal diversity in subjects' neural dynamics Mediano et al. (2020); Schartner et al. (2017) and reduced information transfer between brain regions Barnett et al. (2020). However, in the case of KET, evidence from intracranial recordings in cats suggests a much more complicated picture than that of LSD, with very high variability across individuals, brain regions, and dose levels Pascovich et al. (2021). In a separate line of enquiry, work on EEG data from patients with schizophrenia has also found increased signal diversity Fernández et al. (2011); Li et al. (2008), akin to the effect found under these drugs. Nonetheless, a parsimonious account explaining the similarities and differences between the two states is still lacking.

A promising approach to gain insights into the mechanisms driving the core similarities and differences between psychotomimetic drug states and schizophrenia is to leverage principles from the predictive processing (PP) framework of brain function Clark (2015); Rao and Ballard (1999). A key postulate of the PP framework is that the dynamics of neural populations can be viewed as engaged in processes of inference involving top-down and bottom-up signals. Under this framework, brain activity can be viewed as resulting from a continuous modelling process in which a prior distribution interacts with new observations via incoming sensory information. In accordance with principles of Bayesian inference, discrepancies between the prior distribution and incoming signals (called 'prediction errors') carried by the bottom-up signals drive revisions to the top-down activity, so as to minimize future surprise.

The PP framework has been used to explain perceptual alterations observed in both psychotomimetic drug states Corlett et al. (2009); Leptourgos et al. (2020) as well as in psychiatric illnesses Adams et al. (2016) with a focus on schizophrenia Adams et al. (2013); Brugger and Broome (2018); Fletcher and Frith (2009); Speechley et al. (2010). Most of these accounts of PP are task-based studies, which manipulate stimuli in order to modulate prediction errors. In contrast, here we extend this approach to the resting state, focusing on spontaneous "prediction errors" that arise from naturally occurring neural activity. PP has also been used to understand the action of psychedelics, most notably through the "relaxed beliefs under psychedelics" (or REBUS) model Carhart-Harris and Friston (2019) which posits that psychedelics reduce the precision of prior beliefs encoded in spontaneous brain's activity. REBUS has also been used to inform thinking on the therapeutic mechanisms of psychedelics, where symptomatology can be viewed as pathologically over-weighted beliefs or assumptions encoded in the precision weighting of brain activity encoding them.

To deepen our understanding of the similarities and differences between these conditions, in this paper we replicate and extend findings on neural diversity and information transfer under the two psychotomimetic drugs (LSD and KET) and in schizophrenia using EEG and MEG recordings, and we reproduce these experimental findings as perturbations to a single PP model. Our modelling results reveal that the effects observed under the drugs are indeed reproduced by decreasing the precision-weighting of the priors, while the effects observed under schizophrenia are reproduced by increased precision-weighting of the bottom-up sensory information. Overall, this study puts forward a more nuanced understanding of the relationship between two different psychotomimetic drug states and schizophrenia, and offers a new model-based perspective on how these conditions alter conscious experience.

2. Materials and methods

2.1. Data acquisition and preprocessing

Data from 29 patients diagnosed with schizophrenia and 38 age-matched healthy control subjects were obtained from the Bipolar-Schizophrenia Network on Intermediate Phenotypes (BSNIP) database Tamminga et al. (2013). The subjects were selected within an age range of 20–40 years to match the psychedelic datasets described below. Data included 64-channel EEG recordings sampled at 1000Hz of each subject in eyes-closed resting state, along with metadata about demographics (age and gender), patients' medications and their PANSS symptom scores Kay et al. (1987). The strength of the medication was estimated using the number of antipsychotics taken by each patient (mean: 2.7, range: 0–8), as the dosage of each medication was not available.

Data from healthy subjects under the effects of both drugs was obtained from previous studies with LSD Carhart-Harris et al. (2016b) (N = 17) and ketamine Muthukumaraswamy et al. (2015) (N = 19). Data included MEG recordings from a CTF 275-channel axial gradiometer system with a sampling frequency of 600Hz. Each subject underwent two scanning sessions in eyes-closed resting state: one after drug administration and another after a placebo (PLA).

Preprocessing steps for all datasets were kept as consistent as possible, and were performed using the Fieldtrip Oostenveld et al. (2011) and EEGLAB Delorme and Makeig (2004) libraries. First, the data was segmented into epochs of 2 seconds, and epochs with strong artefacts were removed via visual inspection. Next, muscle and eye movement artefacts were removed using ICA Winkler et al. (2011). Then, a LCMV beamformer Van Veen et al. (1997) was used to reconstruct activity of sources located at the centroids of regions in the Automated Anatomical Labelling (AAL) brain atlas Tzourio-Mazoyer et al. (2002). Finally, source-level data was bandpass-filtered between 1–100Hz, and downsampled with phase correction to 250Hz (EEG) and 300Hz (MEG), and AAL areas were grouped into 5 major Regions of Interest (ROIs): frontal, parietal, occipital, temporal and sensorimotor (see Fig. 1 and Table D.2 in the Appendix). In the rest of the paper we refer to these 5 areas as "ROIs" and to the AAL regions as "sources."

2.2. Analysis metrics

Our analyses are focused on two complementary metrics of neural activity: Lempel-Ziv complexity (LZ) and transfer entropy (TE). Both metrics are based on the same mathematical framework of information theory, and provide characterisations of different but complementary aspects of neural dynamics: LZ captures aspects of the temporal dynamics of *single regions*, while TE quantifies how *different regions influence each other*. Both metrics have a long history, and have been used and robustly validated across a wide range of states of consciousness, including psychedelic states Barnett et al. (2020); Bossomaier et al. (2016); Mediano et al. (2020); Schartner et al. (2017).

Lempel-Ziv complexity (LZ) is a measure of the diversity of patterns observed in a discrete – typically binary – sequence. When applied to neuroimaging data, lower LZ (with respect to wakeful rest) has been associated with unconscious states such as sleep Andrillon et al. (2016) or anaesthesia Zhang et al. (2001), and higher LZ with states of richer phenomenal content under psychedelics, ketamine Mediano et al. (2020);

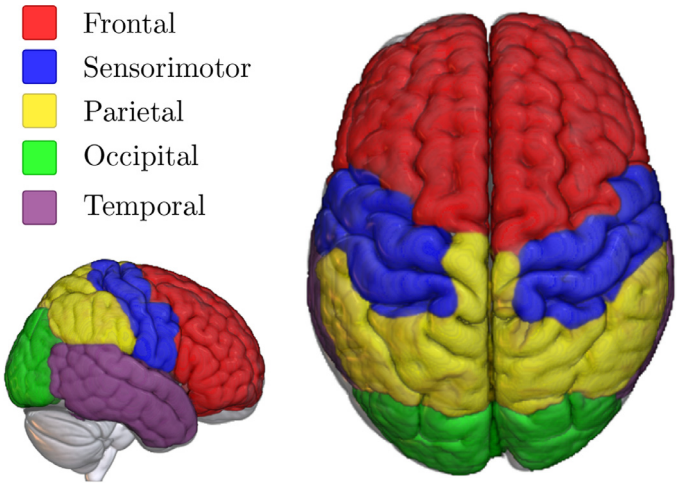

Fig. 1. Regions of interest (ROIs) represented on the MNI-152 standard template. Each ROI is comprised of several regions of the AAL atlas, as per Table D.2.

Schartner et al. (2017) and states of flow during musical improvisation Dolan et al. (2018).

To calculate LZ, first one needs to transform a given signal of length T into a binary sequence. For a given epoch of univariate M/EEG data, we do this by calculating the mean value and transforming each data point above the mean to 1 and each point below to 0. Then, the resulting binary sequence is scanned sequentially using the LZ76 algorithm presented by Kaspar and Schuster Kaspar and Schuster (1987), which counts the number of distinct "patterns" in the signal. Finally, following results by Ziv Ziv (1978), the number of patterns is divided by $\log_2(T)/T$ to yield an estimate of the signal's entropy rate Cover and Thomas (2006), which we refer to generically as LZ. This process is applied separately to each source time series (i.e. to each AAL region), and the resulting values are averaged according to the grouping in Table D.2 to yield an average LZ value per ROI.

In addition to LZ, our analyses also consider transfer entropy (TE) Bossomaier et al. (2016) — an information-theoretic version of Granger causality Barnett et al. (2009) — to assess the dynamical interdependencies between ROIs. The TE from a source region to a target region quantifies how much better one can predict the activity of the target after the activity of the source is known. This provides a notion of directed functional connectivity, which can be used to analyse the structure of large-scale brain activity Barnett et al. (2020); Deco et al. (2021).

Mathematically, TE is defined as follows. Denote the activity of two given ROIs at time t by the vectors $\boldsymbol{X}_t$ and $\boldsymbol{Y}_t$, and the activity of the rest of the brain by $\boldsymbol{Z}_t$. Note that $\boldsymbol{X}_t$, $\boldsymbol{Y}_t$, and $\boldsymbol{Z}_t$ have one component for each AAL source in the corresponding ROI(s). TE is computed in terms of Shannon's mutual information, I, as the information about the future state of the target, $\boldsymbol{Y}_{t+1}$, provided by $\boldsymbol{X}_t$ over and above the information in $\boldsymbol{Y}_t$ and $\boldsymbol{Z}_t$:

$$\mathrm{TE}_{Y\to X|Z} = I(\boldsymbol{X}_t; \boldsymbol{Y}_{t-1}^- \mid \boldsymbol{X}_{t-1}^-, \boldsymbol{Z}_{t-1}^-), \tag{1}$$

where $\boldsymbol{X}_t^-$ refers to the (possibly infinite) past of $\boldsymbol{X}_t$, up to and including time t (and analogously for $\boldsymbol{Y}_t$ and $\boldsymbol{Z}_t$). This quantity can be accurately estimated using state-space models with Gaussian innovations Barnett and Seth (2015), implemented using the MVGC toolbox Barnett and Seth (2014). Note that, when calculating the TE between ROIs, we consider each ROI as a vector — without averaging the multiple AAL sources into a single number. The result is a directed 5×5 network of conditional TE values between pairs of ROIs, which can be tested for statistical differences across groups.

2.3. Statistical analysis

For both LSD and KET datasets, since the same subjects were monitored under both drug and placebo conditions, average subject-level differences (either in LZ or TE) were calculated for each subject, and one-sample t-tests were used on those differences to estimate the effect of the drug.

For the data of patients and controls in the schizophrenia dataset, group-level differences were estimated via linear models. These models used either LZ or TE as target variable, and condition (schizophrenia or healthy), age, gender, and number of antipsychotics (set to zero for healthy controls) as predictors. Motivated by previous work suggesting a quadratic relationship between complexity and age Gauvrit et al. (2017), each model was built with either a linear or quadratic dependence on age, and the quadratic model was selected if it was preferred over a linear model by a log-likelihood ratio test (with a critical level of 0.05).

Finally, multiple comparisons when comparing TE values across all pairs of ROIs were addressed by using the Network-Based Statistic (NBS) Zalesky et al. (2010) method, which identifies 'clusters' of differences – i.e. connected components where a particular null hypothesis is consistently rejected while controlling for family-wise error rate. Our analysis used an in-house adapted version of NBS that works on directed networks, such as the ones provided by TE analyses.

2.4. Computational modelling

A computational model was developed in order to interpret the LZ and TE findings observed on the neuroimaging data. Building on *predictive processing* principles Rao and Ballard (1999), we constructed a Bayesian state-space model that provides an idealised common ground to contrast the three studied conditions – the psychotomimetic drug states, schizophrenia, and baseline (i.e. healthy controls). Our modelling is based on the postulate that the activity of neuronal populations across the brain can be interpreted as carrying out inference on the causes of their afferent signals. Following this view, the proposed model considers the following elements:

- the internal state of a low-level region (i.e. near the sensory periphery), denoted by s_t;
- the internal state of neural activity taking place functionally one level above, denoted by h_t;
- the signal generated at the high-level region in the form of a prediction of the low-level activity, denoted by $\hat{s}_t$;
- the signal generated at the low-level region in the form of a prediction error ξ_t; and
- the precision of the prior λ_p and precision of sensory/afferent information λ_s.

This model represents neural activity within a larger hierarchical processing structure, as illustrated in Fig. 2. The key principle motivating this model is that minimisation of prediction error signals throughout the hierarchy, by updating top-down predictions, implements a tractable approximation to Bayesian inference.[2]

Within this model, we represent the schizophrenia and psychedelic conditions as different types of disruption to Bayesian inference. To describe the psychedelic state, we build on the REBUS hypothesis Carhart-Harris and Friston (2019), which posits a reduced precision-weighting of prior beliefs, leading to increased bottom-up influence.

Conversely, to describe schizophrenia we build on the canonical predictive processing account of psychosis in schizophrenia Sterzer et al. (2018), which postulates an increased precision

[2] Note that in the simple scenario of Eqs. (3), with a single level and Gaussian distributions, inference is in fact exact. In larger or more complicated models inference is often carried out only approximately Gershman (2019).

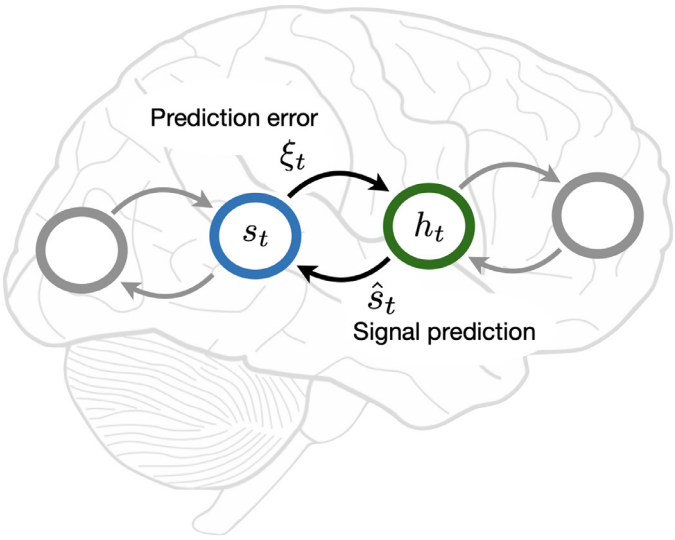

Fig. 2. Graphical illustration of the predictive processing model. The activity of a high-level neural population is represented as a prediction $\hat{s}_t$, and the activity of a low-level population as a prediction error ξ_t. The internal states of the high- and low-level regions are captured by s_t and h_t, respectively.

of sensory input, along with decreased precision of prior beliefs Adams et al. (2016); Fletcher and Frith (2009). Therefore, both conditions are similar in that there is a relative strengthening of bottom-up influence, although instantiated in different ways – which, as shown in Section 3.3, bears important consequences for the behaviour of the model.

It is important to note that predictive processing accounts of schizophrenia remain hotly debated, with other works proposing an increase of prior precision (instead of decrease) as a model of auditory and visual hallucinations Corlett et al. (2019); Teufel et al. (2015). Recent reviews Sterzer et al. (2018) have attempted to reconcile both views by suggesting that sensory hallucinations may be caused by stronger priors, while hallucinations related to self-generated phenomena (like inner speech or self-attention Schneider et al. (2008)) may stem from weaker priors. Here, we base our modelling of SCZ on the weak prior hypothesis, as described above – we return to this issue in this discussion.

To simulate the aberrant dynamics of the inference process, as described above, we consider a given afferent signal (s_t) and construct the corresponding activity of a higher area (h_t), prediction ($\hat{s}_t$), and prediction error (ξ_t), building on the rich literature of state-space models in neuroscience Dayan and Jyu (2003); Dayan et al. (2000); Ratcliff and Rouder (1998). Specifically, we use the linear stochastic process:

$$h_t = ah_{t-1} + \epsilon_t \tag{2a}$$

$$s_t = bh_t + \nu_t \tag{2b}$$

where a, b are weights, and ϵ_t, ν_t are zero-mean Gaussian terms with precision (i.e. inverse variance) λ_p and λ_s, respectively. Note that this formulation is equivalent to

$$h_t|h_{t-1} \sim \mathcal{N}(ah_{t-1}, \lambda_\mathrm{p}^{-1}) \tag{3a}$$

$$s_t|h_t \sim \mathcal{N}(bh_t, \lambda_\mathrm{s}^{-1}). \tag{3b}$$

As we show in the following, λ_p corresponds to the precision of the prior and λ_s to the precision of sensory/afferent information.

The dynamics of this system can be described as a recurrent update between predictions and prediction errors as follows. Eq. (3b) implies that the internal state h_t generates a prediction about the low-level activity given by $\hat{s}_t = bh_t$. At the same time, the dynamics of the high-level region can be seen as a Bayesian update of h_t given s_t and h_{t-1}. Under some simplifying assumptions, the mean of the posterior distribution of h_{t+1} (denoted by $\hat{h}_{t+1}$) is equal to (see Appendix A)

$$\hat{h}_{t+1} = a\hat{h}_t + \beta\xi_t \tag{4}$$

which effectively combines a *prior* $a\hat{h}_t$ (which is the optimal prediction of h_{t+1} given only $\hat{h}_t$, as seen from Eq. (3a)) and a *likelihood* given by the prediction error $\xi_t = s_t - b\hat{h}_t$ that is precision-weighted via β, a parameter known as the *Kalman gain* Durbin and Koopman (2012).

In our simulations, the model is first calibrated using as afferent signals (i.e. s_t) data from the primary visual cortex, corresponding to epochs randomly sampled from the placebo conditions in the LSD and KET datasets. This calibration results in the estimation of the model parameters $a^\mathrm{con}, b^\mathrm{con}, \lambda_\mathrm{p}^\mathrm{con}, \lambda_\mathrm{s}^\mathrm{con}$ for the control condition, which is done using the well-known expectation-maximisation algorithm Moon (1996). With these, the schizophrenia condition is then modelled by setting

$$\lambda_\mathrm{p}^\mathrm{scz} = \lambda_\mathrm{p}^\mathrm{con} \quad \text{and} \quad \lambda_\mathrm{s}^\mathrm{scz} = \eta\lambda_\mathrm{s}^\mathrm{con}, \tag{5}$$

where $\eta > 1$ is referred to as a *noise factor*. This increase of λ_s induces a strengthening of bottom-up prediction errors, and makes the posterior of h_t excessively precise. Conversely, the drug condition is modelled by setting

$$\lambda_\mathrm{p}^\mathrm{psy} = \frac{\lambda_\mathrm{p}^\mathrm{con}}{\eta} \quad \text{and} \quad \lambda_\mathrm{s}^\mathrm{psy} = \lambda_\mathrm{s}^\mathrm{con}. \tag{6}$$

Reducing λ_p also increases the influence of prediction errors, but reduces the precision of the posterior of h_t. Subsequently, for both conditions the parameters a, b are retrained with another pass of the expectation-maximisation algorithm on the placebo trials.

Finally, to compare the model with the empirical M/EEG data, the LZ of the neural activity elicited in the low-level area (i.e. the prediction errors, ξ_t) and the top-down transfer entropy (from the high-level activity $\hat{s}_t$ towards the low-level activity ξ_t) are calculated for each of these three models (control, schizophrenia, and drug).

3. Results

3.1. LSD, KET and schizophrenia all show increased LZ

We begin the analysis by comparing changes in signal diversity, as measured by LZ, across the LSD, ketamine (KET), and schizophrenia (SCZ) datasets.

Our results show strong and significant increases in LZ in all three datasets (Fig. 3), in line with previous work Fernández et al. (2011); Li et al. (2008); Mediano et al. (2020); Schartner et al. (2017). In all three cases the LZ increases are widespread throughout the brain, with the effects in schizophrenia patients being more pronounced in frontal and parietal regions. While the t-scores are higher in LSD and KET than schizophrenia, this could be due to the within-subjects design of both drug experiments – which are more statistically powerful than the between-subjects analysis used on the schizophrenia dataset.

Interestingly, we found that controlling for the medication status of each schizophrenia patient was crucial to obtain results that match prior work Fernández et al. (2011). A direct comparison of LZ values between patients and controls yielded no significant differences ($t = -0.38$, $p = .70$); however, when using a linear model correcting for age, gender, and number of antipsychotics, the antipsychotics coefficient of the model reveals a negative effect on LZ ($\beta = -0.016$, $t = -2.3$, $p = .021$). Additionally, a two-sample t-test calculated between the corrected LZ values of patients and controls yields a substantial difference ($t = 3.4$, $p = .001$). Nonetheless, the sensitivity of this result to these preprocessing steps, as well as the lack of detailed dosage data for each medication, mean it should be considered preliminary and could only be properly interpreted after further investigation in future research (see the corresponding discussion in Section 4.3).

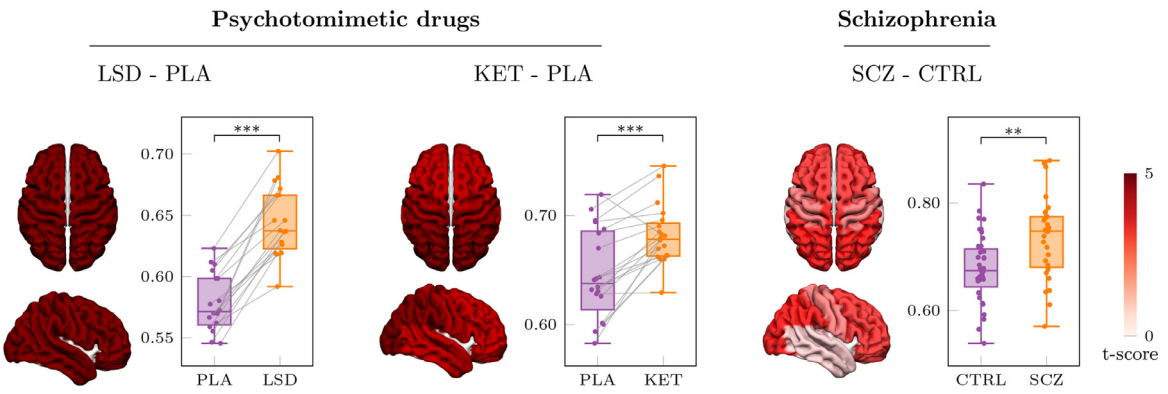

Fig. 3. Increased signal diversity in subjects under the effects of psychotomimetic drugs and in schizophrenia patients. LZ changes are widespread across all ROIs in the three datasets. For the schizophrenia dataset, LZ values shown are corrected for age, gender, and the number of antipsychotic medications taken by each patient using a linear model.

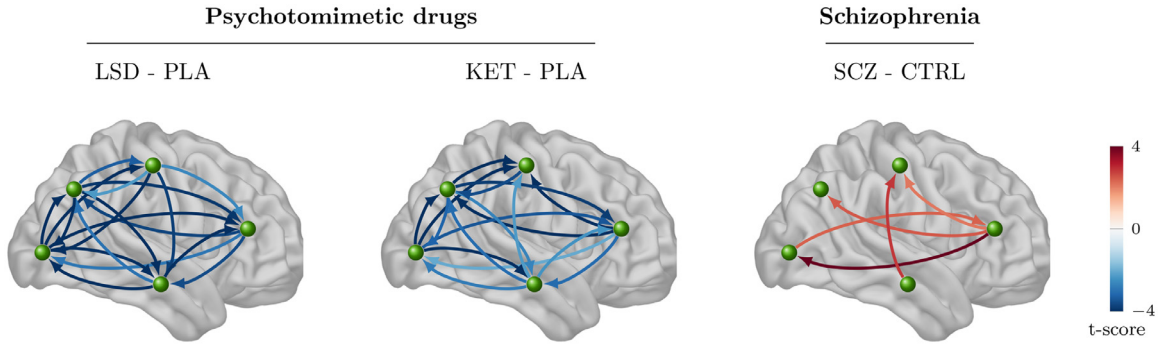

Fig. 4. Lower information transfer under LSD and ketamine but higher information transfer for schizophrenia patients. Transfer entropy (TE) shows a strong widespread decrease in subjects under the effect of LSD or ketamine (KET), compared to a placebo. Conversely, schizophrenia (SCZ) patients show an increase in TE with respect to controls (CTRL), especially from the frontal region to the rest of the brain (controlling for age, gender and antipsychotic use). Links shown are significant after multiple comparisons correction.

3.2. Opposite effect of psychotomimetic drugs and schizophrenia on information transfer

We next report the effects of LSD, KET, and schizophrenia on large-scale information flow in the brain, as measured via transfer entropy (TE). The TE between each pair of ROIs (conditioned on all other ROIs) is calculated for each subject, and used to build directed TE networks. The resulting networks were tested for differences between the drug states and placebo conditions (for LSD and KET), and between patients and controls (for SCZ), correcting for multiple comparisons via cluster permutation testing (see Section 2.3).

We found a ubiquitous decrease in the TE between most pairs of ROIs under LSD and KET (Fig. 4), which is consistent with previous findings Barnett et al. (2020). In contrast, SCZ patients exhibit marked localised increases in TE – and no decreases – with respect to the control subjects. Notably, most increases in TE originated in the frontal ROI, and are strongest between the frontal and occipital ROIs. The increase of information transfer seen in schizophrenia patients therefore takes place "front to back" – aligned with the pathways thought to carry top-down information in the brain from highly cognitive, decision-making regions to unimodal regions closer to the sensory periphery.

As was the case for LZ, controlling for antipsychotic use was key to revealing differences between the healthy controls and schizophrenia patients. In addition, we found a small negative correlation between antipsychotic use and TE between certain ROI pairs – but, unlike for LZ, this effect did not survive correction for multiple comparisons. Although we find significant increase in both LZ and TE between certain regions among the schizophrenia patients when compared to healthy controls, these are not correlated with the symptom scores within the schizophrenia cohort. (see the corresponding discussion in Section 4.3).

3.3. Computational model reproduces experimental results

So far, we have seen that subjects under the effects of two different psychotomimetic drugs display increased signal diversity and reduced information flow in their neural dynamics. In comparison, schizophrenia patients display increased complexity but also increased information flow with respect to healthy controls. We now show how complementary perturbations to the precision terms of the predictive processing model introduced in Section 2.4 reproduce these findings.

We compared the basline model against the drug and schizophrenia variants by systematically increasing the noise factor η, which results in reduced prior precision in the drug model, and increased sensory precision in the schizophrenia model. We then computed the corresponding LZ and TE based on the model-generated time series ξ_t, $\hat{s}_t$ as per Section 2.4 (Fig. 5).

Results show that the proposed model successfully reproduced the experimental findings of both LZ and TE under the two different psychotomimetic drugs and schizophrenia (Fig. 5).

Interestingly, the model also shows (Fig. 5b) that a relative strengthening of sensory information (via either increased sensory precision, or decreased prior precision) can trigger either an increase or a decrease (respectively) of top-down transfer entropy. This suggests that transfer entropy changes cannot be directly interpreted as revealing the changes in any underlying predictive processing mechanisms (see Discussion).

Finally, as a control, we repeated the analysis on the model but exploring the variation of the precision terms in the two unexplored di-

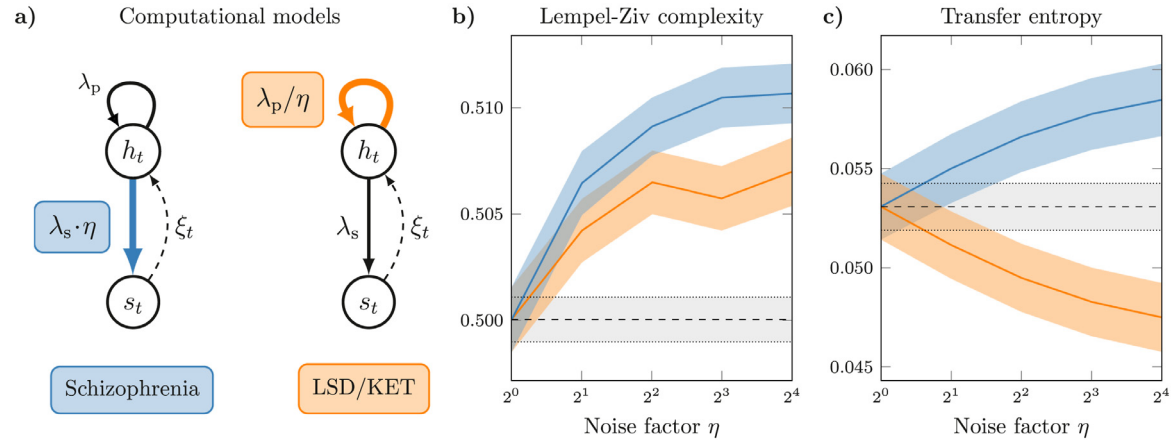

Fig. 5. A computational model based on predictive processing principles reproduces experimental findings in the LSD, ketamine and schizophrenia datasets. (**a**) By increasing the sensory precision (for schizophrenia; **blue**), or reducing the prior's precision (for LSD and KET; **orange**) by a given 'noise' factor η, the model can reproduce the experimental findings of (**b**) increased in LZ in both conditions, and (**c**) opposite changes in TE in both conditions, compared to a baseline (grey). (For interpretation of the references to colour in this figure legend, the reader is referred to the web version of this article.)

rections — either reducing λ_p or increasing λ_s (see Section 2.4). Neither of these changes reproduced the experimental findings (Supp. Fig. B.6), which highlights the specificity of the modelling choices.

4. Discussion

In this paper we have analysed MEG data from healthy subjects under the effects of the psychotomimetic drugs LSD and ketamine, as well as EEG data from a cohort of schizophrenia patients and healthy control subjects. We focused on signal diversity and information transfer, both widely utilised metrics which provide a complementary account of neural dynamics. We found that all datasets show increases in signal diversity, but diverging changes in information transfer, which was higher in schizophrenia patients but lower for subjects under the effects of either drug. In addition to replicating previous results reporting signal diversity and information transfer under the effects of both drugs Barnett et al. (2020); Mediano et al. (2020); Schartner et al. (2017), we described new findings applying these metrics to schizophrenia.

Using a computational model inspired by predictive processing principles Keller and Mrsic-Flogel (2018); Rao and Ballard (1999), we showed that this combination of effects can be reproduced via specific alterations to prediction updating, which can be interpreted as specific forms of disruption to Bayesian inference. Critically, the effects of both psychotomimetic drugs and schizophrenia, on both signal diversity and information transfer, are explained by a relative strengthening of sensory information over prior beliefs, although triggered by different mechanisms – a decrease in the precision of priors in the case of psychotomimetic drugs (consistent with Ref. Carhart-Harris and Friston (2019)), and an increase in the precision of sensory information for schizophrenia.

4.1. Increased sensory precision in schizophrenia

The idea that the symptoms of schizophrenia can be understood as alterations to processes of Bayesian inference has been particularly fertile in the field of computational psychiatry Adams et al. (2016). In particular, various studies based on PP have related psychosis to decreased precision of prior beliefs and increased precision of the sensory inputs Corlett et al. (2009); Fletcher and Frith (2009); Friston et al. (2014); Notredame et al. (2014); Sterzer et al. (2016). These computational models have been supported by a growing number of related experimental findings, including an enhanced confirmation bias Balzan et al. (2013), impaired reversal learning Leeson et al. (2009); Waltz and Gold (2007), and a greater resistance to visual illusions Silverstein and Keane (2011). For instance, schizophrenia patients are less susceptible to the Ebbinghaus illusion, which arises primarily from misleading prior expectations, suggesting that patients do not integrate this prior context with sensory evidence and thus achieve more accurate judgements Horton and Silverstein (2011).

Most of the above mentioned studies are task-based, focusing on differentiating perceptual learning behaviours between healthy controls and schizophrenia patients. Though these studies provide a range of experimental markers, the corresponding methodologies cannot be applied to resting-state or task-free conditions, under which it is known that certain behavioural alterations (e.g. delusions, anhedonia, and paranoia) persist Northoff and Duncan (2016); Northoff and Qin (2011).

The findings presented in this paper provide a step towards bridging this important knowledge gap by providing empirical and theoretical insights into resting-state neural activity under schizophrenia. Although we build on and replicate results related to signal diversity, we are not aware of previous studies of information transfer on schizophrenia in resting state.

4.2. Beyond unidimensional accounts of top-down vs bottom-up processing

The findings presented here link spontaneous brain activity to the PP framework using empirical metrics of signal diversity and information transfer. In the psychotomimetic drug condition, the former increases while the latter decreases; in schizophrenia, both increase – in both cases as compared to baseline placebo or control. The explanation for this pattern of results, articulated by our computational model, is based on the idea that a bias favouring bottom-up over top-down processing can be triggered by changing different precision parameters, which can give rise to opposite effects in specific aspects of the neural dynamics. This observation, we argue, opens the door to more nuanced analyses for future studies.

The increased transfer entropy from frontal to posterior brain areas observed under schizophrenia could be naively interpreted as supporting increased top-down regulation; however, neither the empirical analysis nor the computational model warrant this conclusion. Transfer entropy simply indicates information flow and is agnostic about functional role. Our model-based analyses illustrate how aberrant Bayesian inference in which bottom-up influences become stronger can trigger either an increase or a decrease in transfer entropy from frontal to posterior regions, depending on which precision terms are involved. An interesting possible explanation for this divergence between mechanisms and TE is provided by recent results that show that TE is an aggregate of

qualitatively different *information modes* Mediano et al. (2021b). Future work may explore if resolving TE into its finer constituents might provide a more informative mapping from observed patterns to underlying mechanisms, as well as how these quantities may be related to other consciousness-related electrophysiology metrics Nilsen et al. (2020); Sitt et al. (2014).

Taken together, these findings suggest that conceiving the bottom-up vs top-down dichotomy as a single-dimensional trade-off might be too simplistic, and that multi-dimensional approaches could shed more light on this issue. In particular, our results show how such a simplistic view fails to account for the rich interplay of similarities and differences between schizophrenia and psychosis.

4.3. Limitations and future work

While our empirical and modelling results agree with the canonical PP account of psychosis Sterzer et al. (2018), some reports have suggested a stronger influence of priors over sensory signals – especially in some cases of hallucinations Alderson-Day et al. (2017); Cassidy et al. (2018); Powers et al. (2017). It is important to remark that the 'strengthened prior' interpretation put forward by these task-based studies cannot be accounted for by the simple computational modelling developed here. At the same time, the resting-state model presented here relates spontaneous activity, and our results cannot be directly generalised to task-based settings. Future work may investigate whether a richer hierarchical model is able to reproduce both rest and task data, bridging between these results and prior work.

Regarding the empirical analyses, it is important to note that our analyses are subject to a few limitations due to the nature of the data used. First, the analyses used only 60 AAL sources across 5 ROIs (due to the spatial resolution limitations of EEG), and therefore may neglect potential PP effects that may exist at smaller spatial scales. In addition, the studies on both drugs and schizophrenia used different imaging methods (MEG vs EEG), sampling rate, and experiment designs (within vs between subjects), complicating direct comparisons. Finally, future work should examine how power spectra across the different conditions relate to the findings presented, in terms of both their effect on LZ Mediano et al. (2021c), and their relationship with top-down and bottom-up signalling, for example using band-limited Granger causality Bastos et al. (2015), as well as how directed functional connectivity measures relate to undirected measures such as mutual information and coherence Barnett et al. (2020).

Similarly, while the measures discussed here capture significant differences between schizophrenia patients and healthy controls, more work needs to be done to further characterise the differences within the schizophrenia spectrum, which features a heterogenous array of symptoms and states, e.g. at different phases of the so-called 'psychotic process' Brouwer and Carhart-Harris (2021). A crucial part of this research will be to analyse the clinical symptom scores of the patients and their relationship to both medication and neural dynamics, which was not possible here due to the lack of appropriate metadata on the dosage of antipsychotics. In our preliminary analysis we use the number of antipsychotics as a proxy to the missing dosage data. This proxy measure was found to be negatively correlated with the positive symptom scores of the PANSS scale (see Appendix C) among the schizophrenia patients, suggesting that the symptom scores are confounded by antipsychotic use – but without dosage data it is difficult to disentangle this effect from potential confounds. An interesting possibility is that the neural underpinnings of positive and negative symptoms could be different Fletcher and Frith (2009), and investigating these differences may yield further insight into schizophrenia itself and its relationship with the psychotomimetic drug states. Moreover, both schizophrenia and drug-induced states can be conceived of as dynamic states of consciousness, comprised of several sub-states and/or episodes with hallucinations, delusions and negative symptoms varying widely between and within individuals. Future studies could explore these finer fluctuations in conscious state Mediano et al. (2021a), as well as what features or episodes overlap in the neural and psychological levels between psychotomimetic drug states and schizophrenia.

Finally, recall that (as described in Section 2.1) we used the number of antipsychotic medications being used by each patient as a proxy measure for their medication load. This is a significant oversimplification, as it ignores the specifics of all drugs and their dose-response effects, and future work with richer datasets should explore in more detail the effects of each particular medication – which would potentially bring more nuance to these analyses. Also, the models used for statistical analysis (as per Section 2.3) are linear and may not capture possible non-linear dependencies between antipsychotic use and its effect on neural dynamics (in our case, LZ or TE). Bearing this caveat in mind, our tentative results in the schizophrenia group suggest that antipsychotic use may bring the patients' neural dynamics closer to the range of healthy controls. This finding should be replicated with more detailed analyses involving dosage information and clinical symptom scores, and, if robust, could potentially be used to investigate the mechanism of action of current antipsychotic drugs.

4.4. Final remarks

In this paper we have contrasted changes in brain activity in individuals with schizophrenia (compared to healthy controls) with changes induced by a classic 5-HT_{2A} receptor agonist psychedelic, LSD, and an NMDA antagonist dissociative, ketamine (compared to placebo). Empirical analyses revealed that both schizophrenia and drug states show an increase in neural signal diversity, but they have divergent transfer entropy profiles. Furthermore, we proposed a simple computational model based on the predictive processing framework Rao and Ballard (1999) that recapitulates the empirical findings through distinct alterations to optimal Bayesian inference. In doing so, we argued that both schizophrenia and psychotomimetic drugs can be described as inducing a stronger "bottom-up" influence of sensory information, but in qualitatively different ways, thus painting a more nuanced picture of the functional dynamics of predictive processing systems. Crucially, the proposed model differs from others in the literature in that it is a model of resting-state (as opposed to task-based) brain activity, bringing this methodology closer to other approaches to neuroimaging data analysis based on complexity science Turkheimer et al. (2021).

Overall, this study illustrates the benefits of combining information-theoretic analyses of experimental data and computational modelling, as well as of integrating datasets from patients with those from healthy subjects. We hope our findings will inspire further work deepening our understanding about the relationship between neural dynamics and high-level brain functions, which in turn may accelerate the development of novel, mechanism-based treatments to foster and promote mental health.

Ethics statement

The LSD study Carhart-Harris et al. (2016b) was approved by the National Research Ethics Service committee London-West London and was conducted in accordance with the revised declaration of Helsinki (2000), the International Committee on Harmonization Good Clinical Practice guidelines, and National Health Service Research Governance Framework. Imperial College London sponsored the research, which was conducted under a Home Office license for research with Schedule 1 drugs. The KET study Muthukumaraswamy et al. (2015) was was approved by a UK National Health Service research ethics committee. The schizophrenia data was collected by the B-SNIP consortium Tamminga et al. (2013).

Data and code availability statement

Raw MEG data for the LSD and KET conditions (and their respective placebo controls) is available in the Harvard Dataverse repository. EEG data from schizophrenia patients and healthy controls was obtained from the BSNIP study, accessed via the NIMH Data Archive. Open-source implementations are available online for all tools used in the study, including LZ (link), TE (link), and NBS (link).

Credit authorship contribution statement

Hardik Rajpal: Conceptualization, Methodology, Software, Formal analysis, Writing – original draft, Writing – review & editing. **Pedro A.M. Mediano:** Conceptualization, Methodology, Software, Formal analysis, Writing – original draft, Writing – review & editing. **Fernando E. Rosas:** Conceptualization, Writing – original draft, Writing – review & editing. **Christopher B. Timmermann:** Writing – review & editing. **Stefan Brugger:** Data curation, Writing – review & editing. **Suresh Muthukumaraswamy:** Data curation, Writing – review & editing. **Anil K. Seth:** Writing – review & editing. **Daniel Bor:** Writing – review & editing. **Robin L. Carhart-Harris:** Data curation, Writing – review & editing. **Henrik J. Jensen:** Supervision, Writing – review & editing.

Acknowledgements

H.R. is supported by the Imperial College President's PhD Scholarship. P.M. and D.B. are funded by the Wellcome Trust (grant no. 210920/Z/18/Z). F.R. is supported by the Ad Astra Chandaria foundation. C.T. is funded by the Psychedelic Research Group, Imperial College London. R.C.-H. is the Ralph Metzner Chair of the Psychedelic Division, Neuroscape at University of California San Francisco. A.K.S. is supported by the European Research Council (Advanced Investigator Grant 101019254.) This work was supported in part by grant MR/N0137941/1 for the GW4 BIOMED MRC DTP, awarded to the Universities of Bath, Bristol, Cardiff and Exeter from the Medical Research Council (MRC)/UKRI (S.B.). The LSD research described here was supported by the Beckley Foundation and Walacea Crowd Funding campaign. We thank Imperial College London's Research Computing Service for the computing facilities. Parts of this work were carried out using the computational facilities of the Advanced Computing Research Centre, University of Bristol.

Appendix A. Further details on the predictive processing model

This appendix outlines how a process of Bayesian inference on the probability distribution described by Eq. (3) can be interpreted in terms of the joint dynamics of prediction and prediction error. This is covered in standard textbooks of time series analysis (e.g. in Ref. Durbin and Koopman (2012)) – however, it is provided here for completeness and accessibility.

As a starting point, we assume that a given brain region is trying to infer the hidden cause h_t of its afferent signal, s_t. The brain can use all the previous signals, $\boldsymbol{s}^{t-1} = (s_1, \dots, s_{t-1})$, to generate an optimal prior estimation of h_t, which is given by $p(h_t|\boldsymbol{s}^{t-1})$. When a new sample s_t is observed, this prior can be updated using Bayes' rule,

$$p(h_t|\boldsymbol{s}^t) = \frac{p(h_t, s_t, \boldsymbol{s}^{t-1})}{p(s_t, \boldsymbol{s}^{t-1})} = \frac{p(s_t|h_t)p(h_t|\boldsymbol{s}^{t-1})}{p(s_t|\boldsymbol{s}^{t-1})}.$$

Note that, while in general computing $p(h_t|\boldsymbol{s}^t)$ can be computationally challenging, when all the distributions in the right-hand side of the equation above are Gaussian (as per Eq. (3)) the posterior is easily calculable – as we explain below.

For consistency with the model in Eq. (2), we assume that $h_t|\boldsymbol{s}^{t-1}$ is a Gaussian random variable with mean $\hat{h}_t$ and variance λ_t^{-1}. By considering $p(h_t|\boldsymbol{s}^{t-1})$ as a prior and $p(s_t|h_t)$ as a likelihood, we can compute the posterior $p(h_t|\boldsymbol{s}^t)$ by using Bayes' rule above for Gaussian variables. In this case, standard results for conditional Gaussian distributions (e.g. Ref. (Durbin and Koopman, 2012, Eq. (4.2))) show that

$$\mathbb{E}[h_t|\boldsymbol{s}^t] = \hat{h}_t + \lambda_t^{-1} b F_t^{-1} \xi_t, \tag{A.1}$$

where $\xi_t = s_t - \mathbb{E}[s_t|\boldsymbol{s}^{t-1}] = s_t - b\hat{h}_t$ is the error in the prediction of s_t given $\boldsymbol{s}^{t-1}$, and $F_t = b^2\lambda_t^{-1} + \lambda_s^{-1}$ is the predictive covariance of s_t given $\boldsymbol{s}^{t-1}$. Then, by using Eq. (3a), one can propagate the prediction in Eq. (A.1) to the next step, and obtain a recurrent update equation for $\hat{h}_t$ given by

$$\hat{h}_{t+1} := \mathbb{E}[h_{t+1}|\boldsymbol{s}^t] = a\mathbb{E}[h_t|\boldsymbol{s}^t] = a\hat{h}_t + \beta_t \xi_t \tag{A.2}$$

where $\beta_t = ab\lambda_t^{-1}F_t^{-1}$ is known as the *Kalman gain* parameter (Durbin and Koopman, 2012, Sec. 4.3) and which, as described in Section 2.4, depends only on its previous value $\hat{h}_{t-1}$ and the prediction error ξ_t.

Furthermore, from the definition of β_t and F_t it can be seen that increasing λ_s leads to a higher β_t, thus increasing the bottom-up influence of prediction errors. A similar argument can be made for the increase of β_t with lower λ_p, although this requires writing a recurrent expression analogous to Eq. (A.2) for λ_t and is more mathematically involved. Interested readers are referred to Section 4.3 of Ref. Durbin and Koopman (2012) for a detailed derivation.

Appendix B. Variations of the model

We explored additional variations of the computational model reported above for completeness of the analysis. In this case, results show that increasing state precision or decreasing sensory precision (both cases of increased top-down influence) lead to decreased LZ in the prediction error signals, as seen in Supp. Fig. B.6. This is in opposition to the empirical findings reported in both the psychedelic Schartner et al. (2017) and the schizophrenia Fernández et al. (2011); Li et al. (2008) literature. Overall, these variations further support that both schizophrenia and psychedelics can be modelled as increased bottom-up influences in the resting state. Nonetheless, we hypothesise that these variations may be used to model other altered states of consciousness that exhibit a decrease in neural signal diversity in resting state condition.

Appendix C. Preliminary analysis of symptom scores

As discussed in the main text, we use the number of antipsychotics as a proxy measure for strength of antipsychotic medication used by the patients – in absence of the data on the dosage used/prescribed to the patients. This proxy measure works well to differentiate the neural activity in terms of LZ complexity and TE between brain regions. However, it is worth mentioning that this measure is not capable of controlling for differences observed within the schizophrenia patients.

For completion, here we present a preliminary analysis of PANSS (Positive And Negative Syndrome Scale) symptom scores, in order to explore their relationship to the number of antipsychotics and the neural measures. Results show that the number of antipsychotics is negatively correlated with the positive scores PANSS scores, but not with any other type of symptoms (see Table C.1). Thus, this suggests that the number of antipsychotics do affect the self reported symptoms, highlighting the role of medications in managing the symptoms.

Appendix D. Table with definition of the selected ROIs

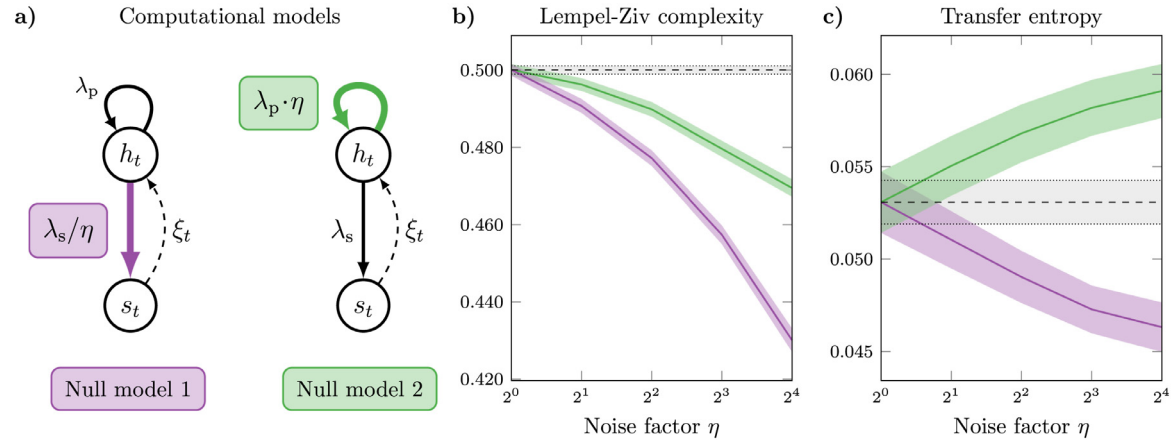

Fig. B1. Computational models with two alternative parametrisations do not reproduce experimental findings. (**a**) We ran the two other possible manipulations of the model, namely decreasing the sensory precision (left; **purple**), or increasing the prior's precision (right; **green**) by a given noise factor η. In both cases the model shows decreased LZ (**b**), contradicting the empirical findings. We also show the model's TE for completeness (**c**).. (For interpretation of the references to colour in this figure legend, the reader is referred to the web version of this article.)

Table C1
>Linear regression results for the symptoms analysis.

Model: Scores ~ 1 + Antipsychotics + Age + Sex		
Score type	Antipsychotics coefficent	
	T value	p value
Positive score	-2.643	0.0082
Negative score	0.224	0.8227
General score	-1.095	0.2731
Total score	-0.983	0.3255

Table D1
Selected regions from the AAL atlas and their corresponding region of interest (ROI).

ROI	AAL indices
Frontal	3–16, 19–20, 23–26
Occipital	43–54
Parietal	59–70
Sensorimotor	1–2, 17–18, 57–58
Temporal	81–90

References

Adams, R.A., Huys, Q.J., Roiser, J.P., 2016. Computational psychiatry: towards a mathematically informed understanding of mental illness. J. Neurol. Neurosurg. Psychiatry 87 (1), 53–63.

Adams, R.A., Stephan, K.E., Brown, H.R., Frith, C.D., Friston, K.J., 2013. The computational anatomy of psychosis. Front. Psychiatry 4, 47.

Alderson-Day, B., Lima, C.F., Evans, S., Krishnan, S., Shanmugalingam, P., Fernyhough, C., Scott, S.K., 2017. Distinct processing of ambiguous speech in people with non-clinical auditory verbal hallucinations. Brain 140 (9), 2475–2489.

Andrillon, T., Poulsen, A.T., Hansen, L.K., Léger, D., Kouider, S., 2016. Neural markers of responsiveness to the environment in human sleep. J. Neurosci. 36 (24), 6583–6596. doi:10.1523/JNEUROSCI.0902-16.2016.

Balzan, R., Delfabbro, P., Galletly, C., Woodward, T., 2013. Confirmation biases across the psychosis continuum: the contribution of hypersalient evidence-hypothesis matches. British Journal of Clinical Psychology 52 (1), 53–69.

Barnett, L., Barrett, A.B., Seth, A.K., 2009. Granger causality and transfer entropy are equivalent for gaussian variables. Phys. Rev. Lett. 103 (23), 238701. doi:10.1103/physrevlett.103.238701.

Barnett, L., Muthukumaraswamy, S.D., Carhart-Harris, R.L., Seth, A.K., 2020. Decreased directed functional connectivity in the psychedelic state. Neuroimage 209, 116462.

Barnett, L., Seth, A.K., 2014. The MVGC multivariate granger causality toolbox: a new approach to granger-causal inference. J. Neurosci. Methods 223, 50–68. doi:10.1016/j.jneumeth.2013.10.018.

Barnett, L., Seth, A.K., 2015. Granger causality for state-space models. Phys. Rev. E 91 (4), 040101. doi:10.1103/PhysRevE.91.040101.

Bastos, A.M., Vezoli, J., Bosman, C.A., Schoffelen, J.-M., Oostenveld, R., Dowdall, J.R., De Weerd, P., Kennedy, H., Fries, P., 2015. Visual areas exert feedforward and feedback influences through distinct frequency channels. Neuron 85 (2), 390–401. doi:10.1016/j.neuron.2014.12.018.

Beck, K., Hindley, G., Borgan, F., Ginestet, C., McCutcheon, R., Brugger, S., Driesen, N., Ranganathan, M., D'Souza, D.C., Taylor, M., et al., 2020. Association of ketamine with psychiatric symptoms and implications for its therapeutic use and for understanding schizophrenia: a systematic review and meta-analysis. JAMA Netw. Open 3 (5). e204693–e204693

Bossomaier, T., Barnett, L., Harré, M., Lizier, J.T., 2016. An introduction to transfer entropy, Vol. 65. Springer.

Brouwer, A., Carhart-Harris, R.L., 2021. Pivotal mental states. J. Psychopharmacol. 35 (4), 319–352. doi:10.1177/0269881120959637.

Brugger, S., Broome, M., 2018. Computational Psychiatry. In: The Routledge Handbook of the Computational Mind. Routledge, pp. 452–468.

Carhart-Harris, R.L., Brugger, S., Nutt, D., Stone, J., 2013. Psychiatry'S next top model: cause for a re-think on drug models of psychosis and other psychiatric disorders. J. Psychopharmacol. 27 (9), 771–778. doi:10.1177/0269881113494107.

Carhart-Harris, R.L., Friston, K., 2019. REBUS And the anarchic brain: toward a unified model of the brain action of psychedelics. Pharmacol. Rev. 71 (3), 316–344.

Carhart-Harris, R.L., Giribaldi, B., Watts, R., Baker-Jones, M., Murphy-Beiner, A., Murphy, R., Martell, J., Blemings, A., Erritzoe, D., Nutt, D.J., 2021. Trial of psilocybin versus escitalopram for depression. N top N. Engl. J. Med. 384 (15), 1402–1411.

Carhart-Harris, R.L., Kaelen, M., Bolstridge, M., Williams, T., Williams, L., Underwood, R., Feilding, A., Nutt, D.J., 2016. The paradoxical psychological effects of lysergic acid diethylamide (LSD). Psychol. Med. 46 (7), 1379–1390. doi:10.1017/S0033291715002901.

Carhart-Harris, R.L., Muthukumaraswamy, S., Roseman, L., Kaelen, M., Droog, W., Murphy, K., Tagliazucchi, E., Schenberg, E.E., Nest, T., Orban, C., et al., 2016. Neural correlates of the LSD experience revealed by multimodal neuroimaging. Proc. Natl. Acad. Sci. 113 (17), 4853–4858.

Carhart-Harris, R.L., Roseman, L., Bolstridge, M., Demetriou, L., Pannekoek, J.N., Wall, M.B., Tanner, M., Kaelen, M., McGonigle, J., Murphy, K., et al., 2017. Psilocybin for treatment-resistant depression: fmri-measured brain mechanisms. Sci. Rep. 7 (1), 1–11.

Cassidy, C.M., Balsam, P.D., Weinstein, J.J., Rosengard, R.J., Slifstein, M., Daw, N.D., Abi–Dargham, A., Horga, G., 2018. A perceptual inference mechanism for hallucinations linked to striatal dopamine. Curr. Biol. 28 (4), 503–514.

Clark, A., 2015. Surfing uncertainty: Prediction, action, and the embodied mind. Oxford University Press.

Corlett, P.R., Frith, C.D., Fletcher, P.C., 2009. From drugs to deprivation: a bayesian framework for understanding models of psychosis. Psychopharmacology (Berl.) 206 (4), 515–530.

Corlett, P.R., Horga, G., Fletcher, P.C., Alderson-Day, B., Schmack, K., Powers III, A.R., 2019. Hallucinations and strong priors. Trends Cogn. Sci. (Regul. Ed.) 23 (2), 114–127.

Cover, T.M., Thomas, J.A., 2006. Elements of information theory. Wiley, Hoboken.

Dayan, P., Jyu, A., 2003. Uncertainty and learning. IETE J. Res. 49 (2–3), 171–181.

Dayan, P., Kakade, S., Montague, P.R., 2000. Learning and selective attention. Nat. Neurosci. 3 (11), 1218–1223.

Deco, G., Vidaurre, D., Kringelbach, M.L., 2021. Revisiting the global workspace orchestrating the hierarchical organization of the human brain. Nat. Hum. Behav. 5 (4), 497–511. doi:10.1038/s41562-020-01003-6.

Delorme, A., Makeig, S., 2004. EEGLAB: An open source toolbox for analysis of single-trial EEG dynamics including independent component analysis. J. Neurosci. Methods 134 (1), 9–21. doi:10.1016/j.jneumeth.2003.10.009.

Dolan, D., Jensen, H.J., Mediano, P.A., Molina-Solana, M., Rajpal, H., Rosas, F., Sloboda, J.A., 2018. The improvisational state of mind: amultidisciplinary study of an improvisatory approach to classical music repertoire performance. Front. Psychol. 9, 1341. doi:10.3389/fpsyg.2018.01341.

Durbin, J., Koopman, S.J., 2012. Time series analysis by state space methods. Oxford University Press.

Fernández, A., López-Ibor, M.-I., Turrero, A., Santos, J.-M., Morón, M.-D., Hornero, R., Gómez, C., Méndez, M.A., Ortiz, T., López-Ibor, J.J., 2011. Lempel–ziv complexity in schizophrenia: a MEG study. Clin. Neurophysiol. 122 (11), 2227–2235.
Fletcher, P.C., Frith, C.D., 2009. Perceiving is believing: a bayesian approach to explaining the positive symptoms of schizophrenia. Nat. Rev. Neurosci. 10 (1), 48–58.
Friston, K., Brown, H.R., Siemerkus, J., Stephan, K.E., 2016. The dysconnection hypothesis (2016). Schizophr. Res. 176 (2–3), 83–94.
Friston, K.J., Stephan, K.E., Montague, R., Dolan, R.J., 2014. Computational psychiatry: the brain as a phantastic organ. Lancet Psychiatry 1 (2), 148–158.
Frohlich, J., Van Horn, J.D., 2014. Reviewing the ketamine model for schizophrenia. J. Psychopharmacol. 28 (4), 287–302.
Gauvrit, N., Zenil, H., Soler-Toscano, F., Delahaye, J.-P., Brugger, P., 2017. Human behavioral complexity peaks at age 25. PLoS Comput. Biol. 13 (4), e1005408. doi:10.1371/journal.pcbi.1005408.
Gershman, S.J., 2019. What does the free energy principle tell us about the brain? Neurons Behav. Data Anal. Theory.
Horton, H.K., Silverstein, S.M., 2011. Visual context processing deficits in schizophrenia: effects of deafness and disorganization. Schizophr. Bull. 37 (4), 716–726.
Kaspar, F., Schuster, H., 1987. Easily calculable measure for the complexity of spatiotemporal patterns. Phys. Rev. A 36 (2), 842. doi:10.1103/PhysRevA.36.842.
Kay, S.R., Fiszbein, A., Opler, L.A., 1987. The positive and negative syndrome scale (panss) for schizophrenia. Schizophr. Bull. 13 (2), 261–276.
Keller, G.B., Mrsic-Flogel, T.D., 2018. Predictive processing: a canonical cortical computation. Neuron 100 (2), 424–435.
Leeson, V.C., Robbins, T.W., Matheson, E., Hutton, S.B., Ron, M.A., Barnes, T.R., Joyce, E.M., 2009. Discrimination learning, reversal, and set-shifting in first-episode schizophrenia: stability over six years and specific associations with medication type and disorganization syndrome. Biol. Psychiatry 66 (6), 586–593.
Leptourgos, P., Fortier-Davy, M., Carhart-Harris, R., Corlett, P.R., Dupuis, D., Halberstadt, A.L., Kometer, M., Kozakova, E., Larøi, F., Noorani, T.N., Preller, K.H., Waters, F., Zaytseva, Y., Jardri, R., 2020. Hallucinations under psychedelics and in the schizophrenia spectrum: an interdisciplinary and multiscale comparison. Schizophr. Bull. 46 (6), 1396–1408. doi:10.1093/schbul/sbaa117.
Li, Y., Tong, S., Liu, D., Gai, Y., Wang, X., Wang, J., Qiu, Y., Zhu, Y., 2008. Abnormal EEG complexity in patients with schizophrenia and depression. Clin. Neurophysiol. 119 (6), 1232–1241.
McCutcheon, R.A., Krystal, J.H., Howes, O.D., 2020. Dopamine and glutamate in schizophrenia: biology, symptoms and treatment. World Psychiatry 19 (1), 15–33.
Mediano, P., Ikkala, A., Kievit, R.A., Jagannathan, S.R., Varley, T.F., Stamatakis, E.A., Bekinschtein, T.A., Bor, D., 2021. Fluctuations in neural complexity during wakefulness relate to conscious level and cognition. bioRxiv doi:10.1101/2021.09.23.461002.
Mediano, P.A., Rosas, F.E., Luppi, A.I., Carhart-Harris, R.L., Bor, D., Seth, A.K., Barrett, A.B., 2021. Towards an extended taxonomy of information dynamics via integrated information decomposition. arXiv preprint arXiv:2109.13186.
Mediano, P.A., Rosas, F.E., Timmermann, C., Roseman, L., Nutt, D.J., Feilding, A., Kaelen, M., Kringelbach, M.L., Barrett, A.B., Seth, A.K., et al., 2020. Effects of external stimulation on psychedelic state neurodynamics. bioRxiv doi:10.1101/2020.11.01.356071.
Mediano, P.A.M., Rosas, F.E., Barrett, A.B., Bor, D., 2021. Decomposing spectral and phasic differences in nonlinear features between datasets. Phys. Rev. Lett. 127 (12), 124101. doi:10.1103/PhysRevLett.127.124101.
Moon, T.K., 1996. The expectation-maximization algorithm. IEEE Signal Process. Mag. 13 (6), 47–60.
Muthukumaraswamy, S.D., Shaw, A.D., Jackson, L.E., Hall, J., Moran, R., Saxena, N., 2015. Evidence that subanesthetic doses of ketamine cause sustained disruptions of NMDA and AMPA-mediated frontoparietal connectivity in humans. J. Neurosci. 35 (33), 11694–11706.
Nichols, D.E., 2004. Hallucinogens. Pharmacol. Therapeutic. 101 (2), 131–181.
Nilsen, A. S., Juel, B., Thürer, B., Storm, J. F., 2020. Proposed EEG measures of consciousness: A systematic, comparative review..
Northoff, G., Duncan, N.W., 2016. How do abnormalities in the brain's spontaneous activity translate into symptoms in schizophrenia? from an overview of resting state activity findings to a proposed spatiotemporal psychopathology. Prog. Neurobiol. 145, 26–45.
Northoff, G., Qin, P., 2011. How can the brain's resting state activity generate hallucinations? a 'resting state hypothesis' of auditory verbal hallucinations. Schizophr. Res. 127 (1–3), 202–214.
Notredame, C.-E., Pins, D., Deneve, S., Jardri, R., 2014. What visual illusions teach us about schizophrenia. Front. Integr. Neurosci. 8, 63.
Oostenveld, R., Fries, P., Maris, E., Schoffelen, J.-M., 2011. Fieldtrip: open source software for advanced analysis of MEG, EEG, and invasive electrophysiological data. Comput. Intell. Neurosci. 2011, 1:1–1:9. doi:10.1155/2011/156869.
Pascovich, C., Castro-Zaballa, S., Mediano, P.A., Bor, D., Canales-Johnson, A., Torterolo, P.D., Bekinschtein, T.A., 2021. Ketamine and sleep modulate neural complexity dynamics in cats. bioRxiv doi:10.1101/2021.06.25.449513.
Powers, A.R., Mathys, C., Corlett, P.R., 2017. Pavlovian conditioning–induced hallucinations result from overweighting of perceptual priors. Science 357 (6351), 596–600.
Rao, R.P., Ballard, D.H., 1999. Predictive coding in the visual cortex: afunctional interpretation of some extra-classical receptive-field effects. Nat. Neurosci. 2 (1), 79–87. doi:10.1038/4580.
Ratcliff, R., Rouder, J.N., 1998. Modeling response times for two-choice decisions. Psychol. Sci. 9 (5), 347–356.
Schartner, M.M., Carhart-Harris, R.L., Barrett, A.B., Seth, A.K., Muthukumaraswamy, S.D., 2017. Increased spontaneous MEG signal diversity for psychoactive doses of ketamine, LSD and psilocybin. Sci. Rep. 7, 46421.
Schneider, F., Bermpohl, F., Heinzel, A., Rotte, M., Walter, M., Tempelmann, C., Wiebking, C., Dobrowolny, H., Heinze, H., Northoff, G., 2008. The resting brain and our self: self-relatedness modulates resting state neural activity in cortical midline structures. Neuroscience 157 (1), 120–131.
Silverstein, S.M., Keane, B.P., 2011. Perceptual organization impairment in schizophrenia and associated brain mechanisms: review of research from 2005 to 2010. Schizophr. Bull. 37 (4), 690–699.
Sitt, J.D., King, J.-R., El Karoui, I., Rohaut, B., Faugeras, F., Gramfort, A., Cohen, L., Sigman, M., Dehaene, S., Naccache, L., 2014. Large scale screening of neural signatures of consciousness in patients in a vegetative or minimally conscious state. Brain 137 (8), 2258–2270.
Speechley, W.J., Whitman, J.C., Woodward, T.S., 2010. The contribution of hypersalience to the "jumping to conclusions" bias associated with delusions in schizophrenia. J. Psychiatry Neurosci.: JPN 35 (1), 7.
Sterzer, P., Adams, R.A., Fletcher, P., Frith, C., Lawrie, S.M., Muckli, L., Petrovic, P., Uhlhaas, P., Voss, M., Corlett, P.R., 2018. The predictive coding account of psychosis. Biol. Psychiatry 84 (9), 634–643.
Sterzer, P., Mishara, A.L., Voss, M., Heinz, A., 2016. Thought insertion as a self-disturbance: an integration of predictive coding and phenomenological approaches. Front. Hum. Neurosci. 10, 502.
Tamminga, C.A., Ivleva, E.I., Keshavan, M.S., Pearlson, G.D., Clementz, B.A., Witte, B., Morris, D.W., Bishop, J., Thaker, G.K., Sweeney, J.A., 2013. Clinical phenotypes of psychosis in the bipolar-schizophrenia network on intermediate phenotypes (B-SNIP). Am. J. Psychiatry 170 (11), 1263–1274.
Teufel, C., Subramaniam, N., Dobler, V., Perez, J., Finnemann, J., Mehta, P.R., Goodyer, I.M., Fletcher, P.C., 2015. Shift toward prior knowledge confers a perceptual advantage in early psychosis and psychosis-prone healthy individuals. Proc. Natl. Acad. Sci. 112 (43), 13401–13406.
Turkheimer, F.E., Rosas, F.E., Dipasquale, O., Martins, D., Fagerholm, E.D., Expert, P., Váša, F., Lord, L.-D., Leech, R., 2021. A complex systems perspective on neuroimaging studies of behavior and its disorders. The Neuroscientist doi:10.1177/1073858421994784. 1073858421994784
Tzourio-Mazoyer, N., Landeau, B., Papathanassiou, D., Crivello, F., Etard, O., Delcroix, N., Mazoyer, B., Joliot, M., 2002. Automated anatomical labeling of activations in SPM using a macroscopic anatomical parcellation of the MNI MRI single-subject brain. Neuroimage 15 (1), 273–289.
Van Veen, B.D., Van Drongelen, W., Yuchtman, M., Suzuki, A., 1997. Localization of brain electrical activity via linearly constrained minimum variance spatial filtering. IEEE Trans. Biomed. Eng. 44 (9), 867–880.
Vollenweider, F.X., Vollenweider-Scherpenhuyzen, M.F., Bäbler, A., Vogel, H., Hell, D., 1998. Psilocybin induces schizophrenia-like psychosis in humans via a serotonin-2 agonist action. Neuroreport 9 (17), 3897–3902.
Waltz, J.A., Gold, J.M., 2007. Probabilistic reversal learning impairments in schizophrenia: further evidence of orbitofrontal dysfunction. Schizophr. Res. 93 (1–3), 296–303.
Winkler, I., Haufe, S., Tangermann, M., 2011. Automatic classification of artifactual ica–components for artifact removal in eeg signals. Behav. Brain Funct. 7 (1), 1–15.
Zalesky, A., Fornito, A., Bullmore, E.T., 2010. Network-based statistic: identifying differences in brain networks. Neuroimage 53 (4), 1197–1207.
Zhang, X.-S., Roy, R.J., Jensen, E.W., 2001. EEG Complexity as a measure of depth of anesthesia for patients. IEEE Trans. Biomed. Eng. 48 (12), 1424–1433. doi:10.1109/10.966601.
Ziv, J., 1978. Coding theorems for individual sequences. IEEE Trans. Inf. Theory doi:10.1109/TIT.1978.1055911.